



 Cite this: *Chem. Commun.*, 2022, 58, 9770

 Received 8th June 2022,  
Accepted 8th August 2022

DOI: 10.1039/d2cc03239b

rsc.li/chemcomm

## Controlling enzyme reactions by supramolecular protection and deprotection of oligosaccharide substrates†

 Milad Zangiabadi and Yan Zhao \*

**Protection/deprotection is a powerful strategy in the total synthesis of complex organic molecules but similar tools are nearly absent in enzymatic reactions. We here report supramolecular protective receptors that outcompete an enzyme in the binding of oligosaccharides. The strong binding inhibits the enzymatic reaction and addition of an even stronger ligand for the receptor releases the substrate. These receptors could be used to control products from the same substrate/enzyme mixture and regulate enzymatic reactions reversibly.**

Protecting groups are indispensable tools in modern organic synthesis.<sup>1</sup> Although the need for selective protection seems low in enzymatic reactions due to the extraordinary substrate selectivity of enzymes, enzymatic selectivity has its own limitations. Exoglycosidases, for example, hydrolyze glycans typically one residue at a time from the nonreducing end.<sup>2</sup> If one wants to cleave two or three residues at a time, different enzymes would be needed if they exist at all. One way to control enzyme reactions is through compartmentation, which can improve efficiency of cascade reactions of a multienzyme system and limit cross reactivities.<sup>3,4</sup> To control a single-enzyme reaction, we postulated that a supramolecular protective receptor would be sufficient.

Our model substrate for the proposed protection/deprotection is a malto-oligosaccharide and maltase cleaves one glucose residue at a time from its nonreducing end.<sup>5</sup> Supramolecular protectors for peptides have been reported<sup>6–13</sup> but tools for glycans are difficult to obtain due to their much weaker binding.<sup>14,15</sup>

Our glycan-protecting receptors were prepared *via* molecular imprinting,<sup>16–18</sup> which has been used to produce different types of glycan-binding materials.<sup>19–27</sup> To shield part of a glycan

while having the rest accessible to the enzyme, however, the receptor must be nanosized and water-soluble, making traditional imprinting methods unsuitable. Our general method (Scheme 1) starts with solubilization of a suitable template in the mixed micelle of cross-linkable surfactants **1** and **2**, together with divinyl cross-linkers and a hydrophobic radical initiator (2,2-dimethoxy-2-phenylacetophenone or DMPA).<sup>28</sup> With a high local concentration of terminal alkyne and azide, the micellar surface is readily cross-linked by the highly efficient click reaction. UV-irradiation then cross-links the micellar core by free radical polymerization, around the template to form a template-complementary imprinted site. The doubly cross-linked micelle is further functionalized on the surface by click reaction with monoazide **3**, to enhance its hydrophilicity and facilitate purification of the resulting molecularly imprinted nanoparticles (MINPs) by simple solvent washing.

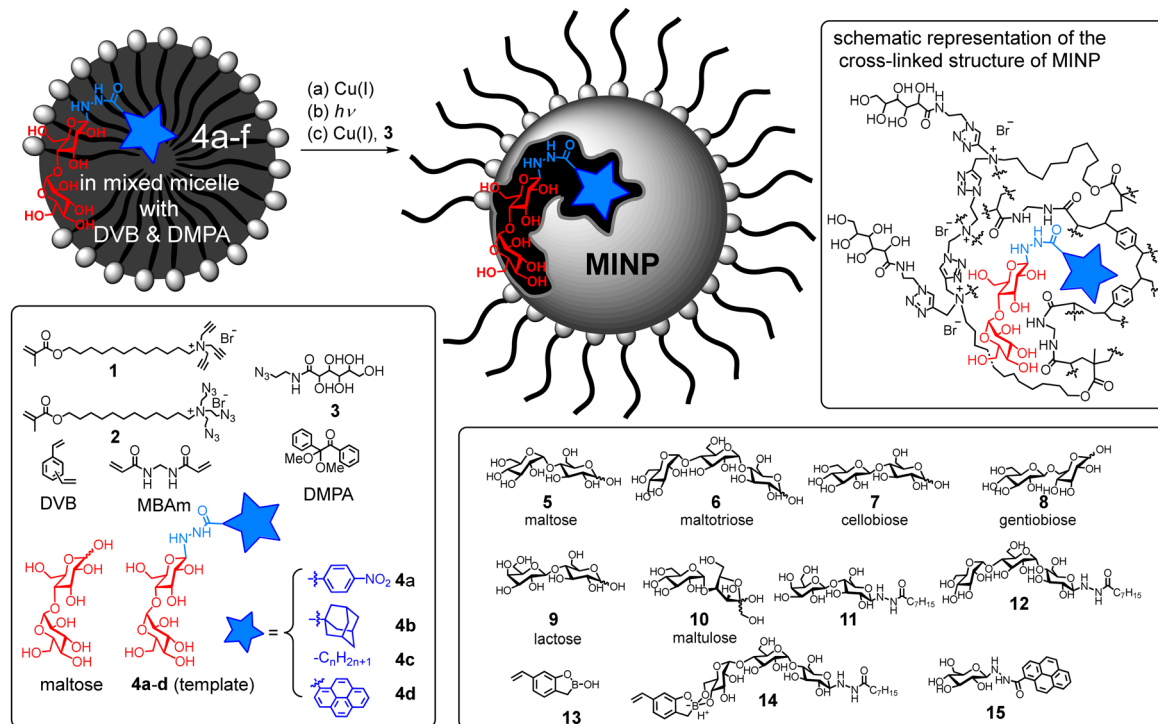
Glycans are strongly solvated in water and thus will not enter a micelle. To help the micelle “catch” the glycan, we converted maltose into neoglycoconjugates **4a–d** as the templates. Amphiphilicity of the templates helps their incorporation into the micelles. Removal of the template after imprinting would “release” the template and allow the imprinted receptor to protect/shield the glycan. We reasoned that the template should work well as a “deprotecting” ligand later on, as it is expected to bind to the MINP protector more strongly than the glycan to be protected.

Natural glycan-binding proteins use an extensive array of hydrogen bonds to bind their guests.<sup>14</sup> To create such a feature in our receptor, we employed a mixture of divinyl benzene (DVB) and *N,N'*-methylenebisacrylamide (MBAm) for the free radical cross-linking. The water-insoluble radical initiator (DMPA) resides inside the micelle. During core-cross-linking, the propagating radical is confined in the micelle and thus could polymerize only those MBAm molecules diffused to surface of the micelle.<sup>29</sup> Cross-linking would fix those MBAm molecules hydrogen-bonded to the template, creating a complementary binding site (Scheme 1, upper right panel). Although hydrogen bonds are compromised by solvent competition for molecular

Department of Chemistry, Iowa State University, Ames, Iowa 50011-3111, USA.

E-mail: zhaoy@iastate.edu; Tel: +1-515-294-5845

 † Electronic supplementary information (ESI) available: Synthetic procedures, characterization data, ITC titration curves, additional data, and NMR spectra. See DOI: <https://doi.org/10.1039/d2cc03239b>

Scheme 1 Preparation of molecularly imprinted nanoparticle (MINP) from a mixed micelle.

recognition in water, they are stabilized inside the hydrophobic core of a micelle<sup>30</sup> or at the surfactant/water interface.<sup>31</sup>

Preparation of the MINPs and their characterization are reported in ESI† The cross-linking was monitored by <sup>1</sup>H NMR spectroscopy (Fig. S1, S3 and S5, ESI†). The particle size was determined by dynamic light scattering (DLS, Fig. S2, S4 and S6, ESI†) and confirmed by transmission microscopy (TEM, Fig. S7, ESI†).

Success of the “catch-and-release” strategy is supported by the strong binding of not only template **4a** but also free maltose by MINP(**4a**)—i.e., MINP prepared with **4a** as the template (Table 1). The binding constant for maltose ( $K_a = 8.4 \times 10^4 \text{ M}^{-1}$ ) compares

favorably with the reported value ( $660 \text{ M}^{-1}$ ) for hydrogen-bond-based small-molecule receptors<sup>32</sup> and is 10–30% of that by maltose-binding periplasmic protein of *Escherichia coli*.<sup>33,34</sup> The binding should be strong enough to outcompete maltase that has a  $K_m$  value of 13.4 mM for maltose and 6.2 mM for maltotriose.<sup>5</sup>

As the acyl group of the template was varied, the MINP receptor bound its own template in the order of **4b** > **4c** ( $n = 7$ ) > **4a**, thus correlating with the overall hydrophobicity of the template. Meanwhile, MINP(**4a–c**) exhibited very similar binding for free maltose (Table 1, entries 2, 4, 6). For template **4c** containing a linear acyl chain, binding of the resulting MINP peaked at C8 (Fig. 1a). When the acyl chain is too short, the hydrophobic driving force most likely is insufficient for the micelle to “catch” the template. When the chain is too long, it

Table 1 Binding of maltose-derived templates and maltose by MINPs determined by isothermal titration calorimetry (ITC)<sup>a</sup>

Entry	Template	Guest	$K_a (\times 10^4 \text{ M}^{-1})$	$-\Delta G (\text{kcal mol}^{-1})$	BR <sup>b</sup>
1	<b>4a</b>	<b>4a</b>	$16.6 \pm 1.3$	7.12	—
2	<b>4a</b>	Maltose	$8.4 \pm 0.4$	6.71	2.0
3	<b>4b</b>	<b>4b</b>	$53 \pm 3$	7.80	—
4	<b>4b</b>	Maltose	$7.0 \pm 0.3$	6.61	7.5
5	<b>4c</b> ( $n = 7$ )	<b>4c</b> ( $n = 7$ )	$32 \pm 2$	7.50	—
6	<b>4c</b> ( $n = 7$ )	Maltose	$9.1 \pm 0.4$	6.76	3.5
7	<b>4d</b>	<b>4d</b>	$862 \pm 11$	9.45	—
8	<b>4d</b>	Maltose	$10.3 \pm 0.6$	6.83	84
9	<b>4d</b>	<b>15</b>	$513 \pm 17$	9.15	50
10	Maltose	Maltose	$\sim 0.003^c$	—	—
11	None	Maltose	$\sim 0.002^c$	—	—

<sup>a</sup> The titrations were performed in duplicates with the indicated errors in HEPES buffer (10 mM, pH 7.4) at 298 K (Fig. S8 and S10, ESI). <sup>b</sup> BR is the binding ratio between the template (or surrogate) to free maltose. <sup>c</sup> The binding constant was estimated from ITC due to the weak binding.

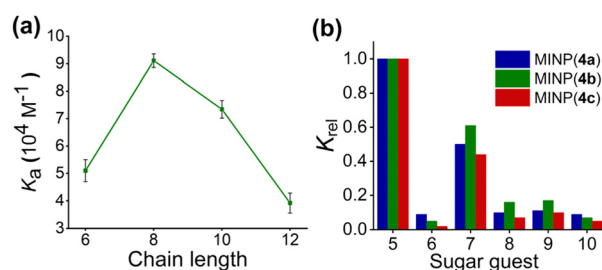


Fig. 1 (a) Dependence of the MINP–maltose binding on the chain length of the acyl group of the template **4c** (Fig. S9, ESI†). (b) Relative binding constants ( $K_{rel}$ ) of different sugars by MINP(**4a–c**) normalized to that of maltose by the same receptor (see Table S1, ESI† for details). The titrations were performed in duplicates in HEPES buffer (10 mM, pH 7.4) at 298 K (Fig. S11–S13, ESI†).



is possible that the glycan gets pushed by the long hydrophobic tail into water while the tail is anchored in the hydrophobic core of the micelle. Since molecular imprinting of the glycan is most effective at the surfactant/water interface (where the majority of MBAm molecules would polymerize), moving the glycan away from this region is expected to be detrimental to the imprinting.

Poor binding was observed when maltose was used directly as the template (entry 10), indicating the importance of the hydrophobic hydrazide in the “catching” of the glycan for imprinting. When the template was eliminated altogether in the preparation, the resulting nonimprinted nanoparticles (NINPs) showed negligible binding (entry 11). The imprinting factor for maltose, measured by the imprint/nonimprint ratio in  $K_a$ , was >3500–4500 for MINP(4a–c).

Among the three receptors, MINP(4c) outperformed the other two in selectivity, evident from its weaker binding of other oligosaccharide guests relative to maltose (Fig. 1b). Among the guests tested (5–10 in Scheme 1), cellobiose (7) showed the highest cross-reactivity (Fig. 1b)—a reasonable result given its structural similarity to maltose. Although the  $\alpha/\beta$  selectivity was modest, the selectivity for chain length (5 vs. 6), glycosylation site (1,4 in 5 vs. 1,6 in 8), and sugar building blocks (5 vs. 9 or 10) was much stronger. One benefit of using hydrogen bonds for sugar binding is their pH-insensitivity. The binding constant for maltose by MINP(4c) stayed largely unchanged over pH 6.5–9 (Fig. S14 and S15, ESI<sup>†</sup>). In contrast, binding between phenylboronic acid and its sugar guests is known to change over an order of magnitude from pH 6.5 to 8.5.<sup>35</sup>

The “catch-and-release” strategy also worked well for other disaccharides, as shown by the molecular imprinting of the lactose-derived template 11 (Table S2, ESI<sup>†</sup>). Poor results were obtained, however, when maltotriose-derived 12 was the template (Table 2). Normally, as long as good host–guest complementary is produced during imprinting, a larger template should afford a stronger binding (to its own imprinted receptor), due to a larger binding interface. However, the binding of the trisaccharide by MINP(12) was less than half of that of the disaccharide by MINP(4c) under comparable conditions ( $K_a = 4.47 \times 10^4$  vs.  $9.1 \times 10^4$  M<sup>-1</sup>). This result suggests that the C8 hydrophobic tail was unable to help the micelle “catch” the glycan effectively. A trisaccharide, having a longer sugar chain, can easily extend itself into the aqueous phase even

while the C8 acyl chain is anchored in the micellar core. Poor imprinting would result as hypothesized earlier when the glycan moves away from the surfactant/water interface.

To better “catch” the trisaccharide, we included boroxole 13 as the functional monomer (FM), which forms anionic boronate 14 *in situ*,<sup>36–38</sup> stabilized by the cationic micelle.<sup>28</sup> With hydrophobic groups at both ends, the amphiphilic template–FM complex should easily migrate into a micelle to be imprinted. MINP(12) prepared with the boroxole FM, indeed, displayed much stronger binding for maltotriose (Table 2), with a binding constant ( $K_a = 33.1 \times 10^4$  M<sup>-1</sup>)  $\sim 1/3$  of that by maltotriose-binding protein of *Thermus thermophilus*.<sup>39</sup> Importantly, the binding selectivity ( $K_{rel}$ ) was maintained while the binding affinity for maltotriose increased.

The strong binding of our MINP receptors allowed them to be used as protective agents for their targeted glycans. Fig. 2a shows that maltase hydrolyzed maltose completely in 20 min in the presence of NINPs. The hydrolysis was measured enzymatically by a commercial glucose assay kit (ESI<sup>†</sup>). In contrast, MINP(14) and, in particular, MINP(4c) inhibited the hydrolysis in a concentration-dependent manner. At a 1 : 1 ratio, the latter was able to suppress the enzymatic hydrolysis to <20%. Not surprisingly, MINP(11) designed for binding lactose gave little protection to maltose.

Not only so, these MINP protectors could be used to alter product distribution in an enzymatic reaction. Fig. 2b shows that maltase hydrolyzed maltotetraose completely into glucose after 2 h with NINPs in the solution. In the presence of 2 equivalents of MINP(4c) ( $n = 7$ ), nearly 40% of the product was maltose. In the presence of MINP(14) designed to shield maltotriose, over 50% of the product was maltotriose. Hence, the MINP protectors were able to shield their targeted glycans and protect them from enzymatic degradation. In this way, different products can be produced with the same substrate and the same enzyme.

The above studies gave us a good understanding of the “catch-and-release” imprinting and yielded strong protectors for both maltose and maltotriose. If we want to deprotect the

Table 2 Binding constants and selectivity of MINP(12)<sup>a</sup>

Entry	Guest	MINP(12)		MINP(12) with FM 13	
		$K_a$ ( $\times 10^4$ M <sup>-1</sup> )	$K_{rel}$	$K_a$ ( $\times 10^4$ M <sup>-1</sup> )	$K_{rel}$
1	Maltotriose	4.47 ± 0.13	1.0	33.1 ± 2.4	1.0
2	Maltose	0.93 ± 0.04	0.21	7.25 ± 0.21	0.22
3	Cellobiose	0.82 ± 0.02	0.18	6.41 ± 0.24	0.19
4	Gentiobiose	0.95 ± 0.06	0.21	7.53 ± 0.13	0.23
5	Lactose	0.81 ± 0.01	0.18	3.44 ± 0.32	0.10
6	Maltulose	0.74 ± 0.05	0.16	5.61 ± 0.25	0.17

<sup>a</sup> The titrations were performed in duplicates with the indicated errors in HEPES buffer (10 mM, pH 7.4) at 298 K (Fig. S17 and S18, ESI).

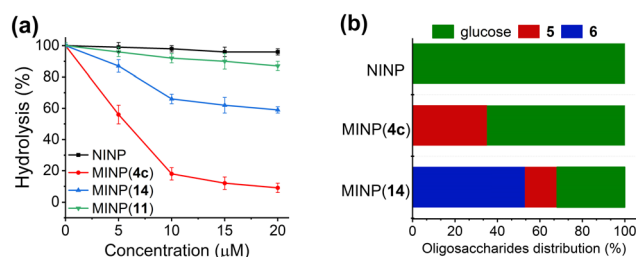


Fig. 2 (a) Hydrolytic yields of maltose after 20 min in 100 mM phosphate buffer (pH 6.8) in the presence of different nanoparticle receptors. MINP(13) was prepared with FM 13. [maltose] = 10 μM. [maltase] = 10 units per mL. (b) Product distribution in the hydrolysis of maltotetraose by maltase in 100 mM phosphate buffer (pH 6.8) after 2 h. [maltotetraose] = 20 μM. [maltase] = 10 units per mL. [nanoparticle] = 40 μM. The product distribution was normalized to “glucose equivalents” by multiplying the concentration of maltose (5) by 2 and the concentration of maltotriose (6) by 3.



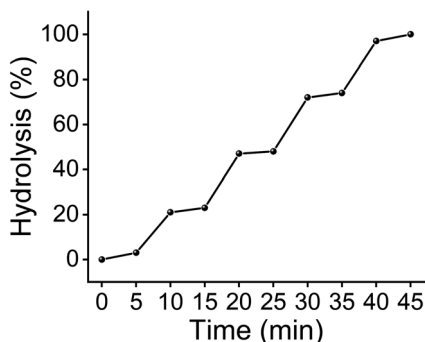


Fig. 3 Hydrolytic yields of maltose over time, with 25  $\mu\text{M}$  of deprotecting ligand **15** added at 5, 15, 25, and 35 min. [maltose] = [MINP(**4d**)] = 100  $\mu\text{M}$ . [maltase] = 10 units per mL.

MINP-bound glycan, however, these MINPs are still lacking, because the template as the deprotecting ligand needs to out-compete the protected glycan in the MINP binding. Yet, the template/glycan binding ratio (BR) was only 2.0–7.5 for MINP(**4a–c**) (Table 1).

Fortunately, to increase the BR value, all we had to do was to use a more hydrophobic hydrazide, since the free sugar does not have the hydrophobic group. Template **4d**, containing a pyrenyl group, afforded a large BR of 84 (Table 1, entry 8). To avoid having the same sugar structure in the deprotecting ligand as in the protected glycan, we synthesized **15**, which has the same pyrene-containing hydrazide conjugated to glucose instead of maltose. With the large hydrophobic pyrenyl group, this template surrogate bound to MINP(**4d**) still much more strongly than maltose, affording a BR of 50 (entry 9).

With a large BR ratio, MINP(**4d**) could be used to protect/deprotect a glycan reversibly. Fig. 3 shows that 1 equivalent of the protective receptor shielded maltose from maltase very well. Anytime when the stronger-binding deprotecting ligand **15** was added, equivalent amounts of maltose were deprotected/released from the MINP protector and underwent enzymatic hydrolysis. The protection/deprotection could be repeated until all the maltose was consumed in the reaction mixture.

Enzymatic reactions in cells are regulated in multiple ways including allosteric, oligomerization, and compartmentation.<sup>40</sup> In this work, we report selective nanoparticle receptors for glycans and demonstrated their abilities to shield the targeted glycans from hydrolytic enzymes. These materials can be used to control product distribution in enzymatic reactions and, in combination with a stronger ligand for the nanoparticles, to modulate enzymatic reactions reversibly.

We thank NSF (DMR2002659) for financial support.

## Conflicts of interest

There are no conflicts to declare.

## Notes and references

1 P. G. M. Wuts, T. W. Greene and T. W. Greene, *Greene's protective groups in organic synthesis*, Wiley, Hoboken, New Jersey, 5th edn, 2014.

- M. Sinnott, *Carbohydrate chemistry and biochemistry: structure and mechanism*, RSC Publishing, Cambridge, 2nd edn, 2013, pp. 299–477.
- A. H. Chen and P. A. Silver, *Trends Cell Biol.*, 2012, **22**, 662–670.
- S. Schmidt, K. Castiglione and R. Kourist, *Chem. – Eur. J.*, 2018, **24**, 1755–1768.
- K. Matsusaka, S. Chiba and T. Shimomura, *Agric. Biol. Chem.*, 1977, **41**, 1917–1923.
- T. Kodadek, *Biopolym. Peptide Sci.*, 2002, **66**, 134–140.
- L. A. Logsdon and A. R. Urbach, *J. Am. Chem. Soc.*, 2013, **135**, 11414–11416.
- E. Faggi, Y. Perez, S. V. Luis and I. Alfonso, *Chem. Commun.*, 2016, **52**, 8142–8145.
- H. Peacock, C. C. Thinnies, A. Kawamura and A. D. Hamilton, *Supramol. Chem.*, 2016, **28**, 575–581.
- J. Mosquera, B. Szyszko, S. K. Y. Ho and J. R. Nitschke, *Nat. Commun.*, 2017, **8**, 14882.
- L. Tapia, N. Solozabal, J. Solà, Y. Pérez, W. T. Miller and I. Alfonso, *Chem. – Eur. J.*, 2021, **27**, 9542–9549.
- X. Li, T. M. Palhano Zanela, E. S. Underbakke and Y. Zhao, *J. Am. Chem. Soc.*, 2021, **143**, 639–643.
- X. Li, K. Chen and Y. Zhao, *Angew. Chem., Int. Ed.*, 2021, **60**, 11092–11097.
- B. Wang and G.-J. Boons, *Carbohydrate recognition: biological problems, methods, and applications*, Wiley, Hoboken, NJ, 2011.
- N. R. Council, *Transforming glycoscience: a roadmap for the future*, National Academies Press, Washington, DC, 2012.
- G. Wulff, *Chem. Rev.*, 2002, **102**, 1–28.
- K. Haupt and K. Mosbach, *Chem. Rev.*, 2000, **100**, 2495–2504.
- L. Ye and K. Mosbach, *Chem. Mater.*, 2008, **20**, 859–868.
- G. Wulff and S. Schauhoff, *J. Org. Chem.*, 1991, **56**, 395–400.
- G. Wulff, *Angew. Chem., Int. Ed. Engl.*, 1995, **34**, 1812–1832.
- S. Wang, D. Yin, W. Wang, X. Shen, J.-J. Zhu, H.-Y. Chen and Z. Liu, *Sci. Rep.*, 2016, **6**, 22757.
- S. Shinde, Z. El-Schich, A. Malakpour, W. Wan, N. Dizayi, R. Mohammadi, K. Rurack, A. Gjörlöf Wingren and B. Sellergren, *J. Am. Chem. Soc.*, 2015, **137**, 13908–13912.
- A. Stephenson-Brown, A. L. Acton, J. A. Preece, J. S. Fossey and P. M. Mendes, *Chem. Sci.*, 2015, **6**, 5114–5119.
- B. Demir, M. M. Lemberger, M. Panagiotopoulou, P. X. Medina Rangel, S. Timur, T. Hirsch, B. Tse Sum Bui, J. Wegener and K. Haupt, *ACS Appl. Mater. Interfaces*, 2018, **10**, 3305–3313.
- J. Pan, W. Chen, Y. Ma and G. Pan, *Chem. Soc. Rev.*, 2018, **47**, 5574–5587.
- Y. Dong, W. Li, Z. Gu, R. Xing, Y. Ma, Q. Zhang and Z. Liu, *Angew. Chem., Int. Ed.*, 2019, **58**, 10621–10625.
- P. X. Medina Rangel, S. Laclef, J. Xu, M. Panagiotopoulou, J. Kovensky, B. Tse Sum Bui and K. Haupt, *Sci. Rep.*, 2019, **9**, 3923.
- R. W. Gunasekara and Y. Zhao, *J. Am. Chem. Soc.*, 2017, **139**, 829–835.
- M. Zangiabadi and Y. Zhao, *Nano Lett.*, 2020, **20**, 5106–5110.
- J. S. Nowick, J. S. Chen and G. Noronha, *J. Am. Chem. Soc.*, 1993, **115**, 7636–7644.
- K. Ariga and T. Kunitake, *Acc. Chem. Res.*, 1998, **31**, 371–378.
- P. Stewart, C. M. Renney, T. J. Mooibroek, S. Ferheen and A. P. Davis, *Chem. Commun.*, 2018, **54**, 8649–8652.
- G. Gilardi, L. Q. Zhou, L. Hibbert and A. E. G. Cass, *Anal. Chem.*, 1994, **66**, 3840–3847.
- M.-H. Seo, J. Park, E. Kim, S. Hohng and H.-S. Kim, *Nat. Commun.*, 2014, **5**, 3724.
- J. Yan, G. Springsteen, S. Deeter and B. Wang, *Tetrahedron*, 2004, **60**, 11205–11209.
- M. Dowlut and D. G. Hall, *J. Am. Chem. Soc.*, 2006, **128**, 4226–4227.
- M. Bérubé, M. Dowlut and D. G. Hall, *J. Org. Chem.*, 2008, **73**, 6471–6479.
- H. Kim, Y. J. Kang, S. Kang and K. T. Kim, *J. Am. Chem. Soc.*, 2012, **134**, 4030–4033.
- M. J. Cuneo, A. Changela, L. S. Beese and H. W. Hellinga, *J. Mol. Biol.*, 2009, **389**, 157–166.
- A. Sols, in *Current Topics in Cellular Regulation*, ed. B. L. Horecker and E. R. Stadtman, Academic Press, 1981, vol. 19, pp. 77–101.

